Molecular Biology of the Cell
Vol. 12, 1147–1160, April 2001

Depletion of Acyl-Coenzyme A-Binding Protein Affects Sphingolipid Synthesis and Causes Vesicle Accumulation and Membrane Defects in *Saccharomyces cerevisiae*

Barbara Gaigg,*† Thomas B. F. Neergaard,*† Roger Schneiter,‡ Jan Krogh Hansen,* Nils J. Færgeman,* Niels A. Jensen,* Jens R. Andersen,* Jørgen Friis,* Roger Sandhoff,§ Henrik Daa Schrøder,‖ and Jens Knudsen*¶

*Department of Biochemistry and Molecular Biology, ‖Institute of Pathology, University of Southern Denmark, Odense University, DK-5230 Odense M, Denmark; ‡Institute of Biochemistry, Graz, University of Technology, A-8010 Graz, Austria; and §German Cancer Research Center, 69120 Heidelberg, Germany

Submitted June 15, 2000; Revised January 29, 2001; Accepted January 30, 2001
Monitoring Editor: Howard Riezman

Deletion of the yeast gene *ACB1* encoding Acb1p, the yeast homologue of the acyl-CoA-binding protein (ACBP), resulted in a slower growing phenotype that adapted into a faster growing phenotype with a frequency $>1:10^5$. A conditional knockout strain (Y700p*GAL1-ACB1*) with the *ACB1* gene under control of the *GAL1* promoter exhibited an altered acyl-CoA profile with a threefold increase in the relative content of C18:0-CoA, without affecting total acyl-CoA level as previously reported for an adapted *acb1*Δ strain. Depletion of Acb1p did not affect the general phospholipid pattern, the rate of phospholipid synthesis, or the turnover of individual phospholipid classes, indicating that Acb1p is not required for general glycerolipid synthesis. In contrast, cells depleted for Acb1p showed a dramatically reduced content of C26:0 in total fatty acids and the sphingolipid synthesis was reduced by 50–70%. The reduced incorporation of [^{3}H]*myo*-inositol into sphingolipids was due to a reduced incorporation into inositol-phosphoceramide and mannose-inositol-phosphoceramide only, a pattern that is characteristic for cells with aberrant endoplasmic reticulum to Golgi transport. The plasma membrane of the Acb1p-depleted strain contained increased levels of inositol-phosphoceramide and mannose-inositol-phosphoceramide and lysophospholipids. Acb1p-depleted cells accumulated 50- to 60-nm vesicles and autophagocytotic like bodies and showed strongly perturbed plasma membrane structures. The present results strongly suggest that Acb1p plays an important role in fatty acid elongation and membrane assembly and organization.

INTRODUCTION

Acyl-CoA binding protein (ACBP) is an 86- to 92-residue protein with a highly conserved sequence found in a wide range of species from yeast and plants to reptiles, birds, and mammals (Kragelund *et al.*, 1996). ACBP homologues can be grouped into four different types: 1) a general basic form (l-ACBP), which is expressed in all tissues in all tested eukaryotes (Kragelund *et al.*, 1999); 2) a testis-specific form (t-ACBP), called endozepin-like protein, which has been shown to be present in spermatozoa only (Pusch *et al.*, 1996); 3) a brain-specific form (Lihrmann *et al.*, 1994); and 4) a group of larger proteins, which contain an ACBP subdomain. The $\Delta^3\Delta^2$-enoyl-CoA isomerase, which is essential for β-oxidation of unsaturated fatty acids in mammalian peroxisomes, belongs to this group (Geisbrecht *et al.*, 1999). The *Caenorhabditis elegans* genome contains six putative open reading frames with partial homologies to ACBP. Bovine ACBP, rat l-ACBP, yeast ACBP, and ACBP from *Arabidopsis thaliana* bind saturated and unsaturated C14–C22-acyl-CoA esters with high specificity and affinity (K_D 1–15 nM; Rosendal *et al.*, 1993; Faergeman *et al.*, 1996; Jens Knudsen, unpublished results). ACBP is unable to bind free fatty acids but binds CoA with a K_D of 1–2 μM (Robinson *et al.*, 1996). The

† These authors contributed equally to the experimental work performed.

¶ Corresponding author. E-mail: jkk@bmb.sdu.dk.

CoA head group thus plays a key role in mediating the specificity for binding of acyl-CoA esters.

Long-chain acyl-CoA esters serve as important intermediates in fatty acid elongation, lipid synthesis, and fatty acid degradation. In addition to these functions, a large body of evidence indicates that long-chain acyl-CoA esters also have important functions in the regulation of intermediary metabolism and transcription (Færgeman and Knudsen, 1997). ACBP has been shown to protect acetyl-CoA carboxylase, acyl-CoA synthetase, and adenylate translocase against inhibition by long-chain acyl-CoA esters in vitro (Rasmussen *et al.*, 1993). ACBP mediates intermembrane acyl-CoA transport and protects long-chain acyl-CoA esters from being hydrolyzed by cellular acyl-CoA hydrolases (Færgeman and Knudsen, 1997). The observation that ACBP can facilitate transport of acyl-CoA between membranes in vitro combined with the fact that overexpression of bovine ACBP in yeast increases the intracellular acyl-CoA pool strongly suggest that ACBP acts as an acyl-CoA transporter and pool former in vivo.

Long-chain acyl-CoA esters have been shown to be required for fission and fusion of COPI-coated vesicles (Glick and Rothman, 1987; Pfanner *et al.*, 1989, 1990; Rothman and Wieland, 1996). Long-chain acyl-CoA esters are also a requisite for the endophilin and CtBP/BARS catalyzed acylation of lysophosphatidic acid (LPA), which is required for the formation of endocytic vesicles and for fission of Golgi membranes, respectively (Schmidt *et al.*, 1999; Weigert *et al.*, 1999).

In the present work we show that yeast cells carrying a deletion in the *ACB1* gene are extremely unstable and revert into a faster growing "adapted" variant with a frequency $>1:10^5$. To circumvent the adaptation problem, we constructed a conditionally Acb1p-depleted strain, in which *ACB1* is under the regulation of the glucose-repressible *GAL1*-promoter (Y700p*GAL1-ACB1*). Under repressing glucose conditions, Y700p*GAL1-ACB1* exhibits reduced growth rate on synthetic medium, changes in acyl-CoA chain length profile, and strongly reduced synthesis of very long-chain fatty acids (VLCFA) and sphingolipids. Under these growth conditions, this strain accumulates 50- to 60-nm vesicles, autophagocytotic-like bodies, and bundles of unidentified fibrous material closely associated with the plasma membrane. These results indicate that abrogated intracellular transport of de novo synthesized acyl-CoA esters in Y700p*GAL1ACB1* strongly affects membrane structure and organization in vivo.

MATERIALS AND METHODS

Yeast Strains and Culture Media

The *Saccharomyces cerevisiae* strain used was Y700: *MATa, ade2-1 trp1 can1-100 leu2-3 leu2-112 his3-11 his3-15 ura3*, a haploid derivative of W303.

Yeast strains were cultivated at 30°C in minimal YNB medium (8 g/l yeast nitrogen base without amino acids [with or without inositol], 55 mg/l adenine, 55 mg/l tyrosine) containing the amino acid mixture and uracil in a 7× concentration. Acb1p-depleted cells used for experiments were maintained on 2% galactose plates. When needed, a colony was picked and diluted to OD 0.005 and grown for 24 h in glucose medium, diluted to OD 0.1 into fresh glucose medium, and grown to the optical density indicated. Where indicated, the cells were supplemented with either 500 μM fatty acid/0.05% Brij58 or 25 μM phytosphingosine (PHS) when diluted into fresh media. If nothing else is stated, cells were kept on YP-galactose plates (2%) and inoculated in YNB medium supplemented with 2% glucose to an OD_{600} of 0.005. Cells were grown for 24 h, diluted into fresh medium to an OD_{600} of 0.05–0.1, and grown to the OD_{600} indicated.

Genetic Manipulations

Disruption of *ACB1* was performed by the one-step gene disruption technique (Rothstein, 1983). The 195-bp *Hin*dII-*Bcl*I fragment of pACB1cer Dbg950 (Borsting *et al.*, 1997) was replaced with the 3.5-kb pair *Sca*I-*Bam*HI fragment covering the *LEU2* gene from the plasmid pRS305 (kindly provided by R. Rothstein). A 3.9-kb pair *Nhe*I/*Ava*I fragment containing the disrupted *ACB1* gene was isolated and used for *ACB1* disruption. The plasmid pFA6a-kanMX4-prom*GAL1* (Wach *et al.*, 1994) containing the kanMX4 resistance marker and the *GAL1* promoter was used as a template for polymerase chain reaction (PCR) to amplify the replacement fragment. A pair of oligonucleotide hybrid oligonucleotides (upstream oligo: CTAAAACTCTAAAATTAGTTAAACTAGTGTTTTCAGCAA AATCGATGAATTCGAGCTCG; downstream oligo: CGTTGACG-GCTTTAGCTTTTTCTTCGAATAATTGGGAAACCATGGATCCG-GGGTTTTTTCTCCT, where the underlined sequences indicate homology to the KanMX4 gene) containing 40 nucleotides homologous to the upstream region or to the first 40 nucleotides of the coding region of *ACB1* and 18–19 nucleotides homologous to pFA6a-kanMX4-prom*GAL1*, was used. The 40 nucleotides homologous to the upstream region of *ACB1* were located immediately upstream of the start codon. PCR fragments of ~1.65 kb, harboring the kanMX4 marker and the *GAL1* promoter and flanking sequences, were generated, using standard techniques with ~50 ng of the *Not*I fragment of pFA6a-kanMX4-prom*GAL1* as a template. Y700 was rendered competent using lithium acetate as described by Gietz *et al.* (1992). Transformants were selected on YP plates supplemented with 2% galactose and 200 μg/ml G418.

Extraction and Analysis of Fatty Acids and Acyl-CoAs

Growth was stopped by addition of 0.1 volume of chilled 6.6 M perchloric acid and crushed ice directly to the medium. Cells (4×10^9) were harvested and washed once with 10 mM perchloric acid. The supernatant was removed and 100–150 μg C15:0 fatty acid and 1 nmol C17:0-CoA were added as internal standards. The volume was adjusted to 250 μl, and 1 g of glass beads was added. The mixture was shaken at 0°C until cells were broken as determined by microscopy. H_2O (0.5 ml) and chloroform:methanol (2:1, 3 ml) were added and mixed. An additional 1 ml of chloroform and 1 ml of H_2O were added and mixed again. The mixture was centrifuged to separate the phases. The lower phase containing the fatty acids was dried under nitrogen. The lipids were hydrolyzed with 0.4 ml of 0.5 M NaOH in methanol at 100°C overnight and methylated with BF_3. The methyl esters were separated on a Chrompak CP-CIL 88 capillary column (Chrompack, Middelburg, the Netherlands) using hydrogen as a carrier gas and a temperature gradient from 145 to 220°C (10°C/min). The acyl-CoA–containing interphase from the lipid extraction was dried under nitrogen. 2-(*N*-morpholino)ethanesulfonic acid (0.7 ml of 100 mM, pH 6.5) containing 0.7 mg of recombinant ACBP was added. The acyl-CoA esters were extracted by shaking for 90 min at 4°C and analyzed by high performance liquid chromatography. The recovery of radioactive C16:0-CoA added together with the C17:0-CoA internal standard was >75%.

Samples were loaded onto a small ODS 10/100 precolumn equilibrated with 20% acetonitrile in 20 mM KH_2PO_4, pH 5.3, and washed for 5 min. The acyl-CoA esters were then eluted in reversed manner on an ODS 10/100 column (4.6 × 250 mm) by the following gradient of solvent B (70% acetonitrile in 20 mM KH_2PO_4, pH 5.3) in solvent A (30% acetonitrile in 20 mM KH_2PO_4, pH 5.3): 15–25% for

25 min, 25–45% for 20 min, 45–65% for 10 min, 65–90% for 6 min, and 90% for 9 min. The flow was 1.0 ml/min.

Phospholipid (PL) Analysis

Determination of steady-state PL composition was done essentially as described by Patton-Vogt *et al.* (1997). Cells were grown in low phosphate synthetic medium containing 10 μCi [^{32}P]P_i/ml for six to seven generations. Lipids were extracted, and individual PLs were resolved by two-dimensional thin-layer chromatography (TLC), using chloroform:methanol:ammonium hydroxide (65:35:7) for the first dimension and chloroform:acetone:methanol:acetic acid:H_2O (10:4:2:2:1) for the second dimension. The plates were scanned on a STORM Phosphor Imager 840 (Molecular Dynamics, Sunnyvale, CA), and spots were quantified using ImageQuant software (Amersham-Pharmacia Biotech, Uppsala, Sweden).

Mass Spectroscopic Analysis of Plasma Membrane Lipids

Plasma membranes were isolated following the procedure described by Serrano (1988). Lipids were extracted and analyzed by mass spectroscopy on a Quattro II (Micromass, Manchester, United Kingdom) as previously described (Schneiter *et al.*, 1999).

Protein Extraction and Western Blotting

Cells were lysed with 0.5 ml of 0.2 M NaOH, 0.2% β-mercaptoethanol for 10 min on ice. Proteins were precipitated with 5% trichloroacetic acid. The pellets were dissolved in 70 μl of 2 volumes of SDS-sample buffer (2×) and 1 volume of 1 M Tris base, heated at 95°C for 10 min, and subjected to 10% SDS-PAGE. Proteins were blotted onto a nitrocellulose membrane (KEM EN TEC, Copenhagen, Denmark) and detected using the enhanced chemiluminescence as described by the manufacturer (Amersham-Pharmacia Biotech, Uppsala, Sweden).

Determination of Acb1p Acyl-CoA–Binding Specificity by Isoelectric Focusing

Isoelectric focusing analysis was performed on a Pharmacia Phast System using pH 3–9 as recommended by the manufacturer. Acyl-CoA esters were synthesized as previously described (Knudsen, 1979). All ligands were in threefold molar excess to yeast ACBP (1 mg/ml).

RNA Preparation

The cells were immediately cooled by addition of 1 volume of ice, pelleted, and washed with ice-cold water. Total RNA was extracted by the hot phenol method, immediately dissolved in freshly deionized formamide, and stored at −80°C.

Northern Blotting

Total RNA (10 μg/lane) was separated on 1% (wt/vol) denaturing agarose gel and transferred to a ZetaProbe GT positive nylon membrane (Bio-Rad, Hercules, CA). Reverse transcription-PCR-generated probes were labeled with [^{32}P]dCTP using an oligolabeling kit (Pharmacia Biotech). The three *ELO* probes were checked for specificity with three corresponding knockout strains (kindly provided by C.E. Martin (*elo1*Δ) and G. Loison (*elo2*Δ/*fen1*Δ and *elo3*Δ/*sur4*Δ)).

Labeling of Total Cellular Sphingolipids with [^{3}H]myo-Inositol

For steady-state labeling cells were grown from OD 0.1 to 0.5 in 3 ml of YNB medium containing 11 μM inositol and 30 μCi [^{3}H]*myo*-inositol (NEN Life Science Products, Boston, MA). For pulse labeling, 40 OD_{600} units of cells were pulsed with 4 μCi [^{3}H]*myo*-inositol per OD in inositol-free medium at OD 10 for 15 min and chased for 5 h.

At the indicated time, the OD_{600} was determined, 1 ml of each of the cultures was chilled on ice, and 5–6 OD units of unlabeled stationary phase cells were added as carrier. The cells were harvested, washed twice with ice-cold H_2O, and resuspended in 5% trichloroacetic acid at 4°C for 20 min. Glass beads (0.5 ml, 425–600 μm) were added, lipids were extracted twice for 30 min at 60°C with 1 ml of ethanol:water:diethyl ether:pyridine:ammonium hydroxide (15:15:5:1:0.018) on a thermomixer at 1400 rpm, extracts were pooled, and the solvent was evaporated. Lipids were dissolved in chloroform:methanol:water (16:16:5), and ^{3}H activity was determined by scintillation counting of 10 μl. Mild saponification was performed with 1 ml of 0.2 M NaOH in methanol at 30°C for 1 h. EDTA (1 ml 0.5 M) was added, the solution was acidified with 200 μl of 1 M acetic acid, and unsaponified lipids were extracted with 1 ml of chloroform. The extracts were dried, the sphingolipids were redissolved in 30 μl of chloroform:methanol (1:1), and incorporated [^{3}H]*myo*-inositol was quantified by scintillation counting. Individual lipid species were separated by high-performance TLC (HPTLC) using chloroform:methanol:4.2 M ammonium hydroxide (9:7:2) as the developing solvent. HPTLC plates were scanned on an Automatic TLC-Linear Analyzer Tracemaster 20 (Berthold, Nashua, NH).

Spheroplast Rate Assay

Cells were harvested, washed three times in deionized water, and resuspended to OD 0.5 in Tris-EDTA buffer (pH 7.3) at 25°C. Freshly prepared Zymolyase 20T (25 μl of 2 mg/ml; Seikagaku, Tokyo, Japan) was added and OD_{600} was determined as indicated.

[^{3}H]myo-Inositol and [^{3}H]Serine Uptake Assay

The cells were diluted in fresh inositol medium (with or without palmitic acid) to an OD_{600} of 0.1 and grown to OD_{600} 0.5. Cells were then washed three times with phosphate-buffered saline (PBS) and resuspended in PBS (30°C) to OD 1.0. Cells (1 ml) were incubated at 30°C for 5 min, and then 10 μCi [^{3}H]*myo*-inositol (NEN Life Science Products, Madison, WI) was added. Incubation was continued with gentle shaking. Samples (200 μl) were collected and transferred to a stop solution on ice (1 ml of ice-cold PBS containing 90 μg of inositol/ml) after 1, 4, 7, and 10 min. Cells were collected on GF/C glass microfiber paper (Whatman Tewksbury, MA), washed three times with ice-cold PBS, and air-dried. [^{3}H]*myo*-inositol uptake was determined using a STORM Phosphor Imager 840 (Molecular Dynamics). Serine uptake was assayed and quantified in a similar manner using 20 μCi [^{3}H]serine (NEN Life Science Products, Boston, MA) and 10 mM serine in the stop buffer.

Electron Microscopy

Electron microscopy was performed as described by Kaiser and Schekman (1990).

RESULTS

Construction of Y700pGAL1-ACB1, a Conditional Y700acb1Δ Strain

We have previously shown that disruption of the *ACB1* gene in three different strains of the yeast *S. cerevisiae* had no effect on the growth rate on YNB-glucose medium (Schjerling *et al.*, 1996; Gaigg, Neergaard, Schneiter, Hansen, Færgeman, Jensen, Andersen, Friis, Sandhoff, Schrøder, and Knudsen, unpublished results). In contrast, Choi *et al.* (1996) showed that disruption of *ACB1* in the wild-type strain DTY10A resulted in retardation of growth compared with wild type. The variable phenotype

of *acb1* null mutant cells could indicate that different genetic backgrounds respond differently to the lack of Acb1p or that the *acb1*Δ strains are unstable and undergo adaptational changes, which enables them to grow faster. A diploid *ACB1/acb1*Δ strain always segregated into two big and two small colonies (with and without the *ACB1* gene, respectively, as confirmed by PCR, Gaigg, Neergaard, Schneiter, Hansen, Færgeman, Jensen, Andersen, Friis, Sandhoff, Schrøder, and Knudsen, unpublished results). When an original *acb1*Δ colony from a transformation or from a tetrad analysis was resuspended and plated on YNB-glucose medium, 1 of 10,000 colonies were significantly larger, i.e., adapted into a faster growing phenotype. Small colonies from this plate, grown in liquid YNB-glucose medium, showed an adaptation frequency of $1:10^4$ to 1:10.

The high adaptation rate of Y700*acb1*Δ made this strain unsuitable to study the physiological function of Acb1p. To construct a condition knockout, we inserted the *GAL1* promoter directly in front of *ACB1* without deleting anything of the original promoter of *ACB1* to avoid interference with the expression of *ORM1*, a gene of ~700 bp upstream of *ACB1*, sharing promoter region with *ACB1*. Northern blotting analysis confirmed that *Y700* and *Y700pGAL1-ACB1* express identical levels of *ORM1* mRNA when grown in YNBD medium with and without 500 μM palmitic acid added, although addition of fatty acids increased *ORM1* mRNA expression 1.7 in both wild-type and the Acb1p-depleted cells (Gaigg, Neergaard, Schneiter, Hansen, Færgeman, Jensen, Andersen, Friis, Sandhoff, Schrøder, and Knudsen, unpublished results). We therefore conclude that Orm1p expression is not affected by depletion of Acb1p in*Y700pGAL1-ACB1.*

When a single colony from a galactose plate was grown in media supplemented with 2% galactose for 36 h, Y700 and Y700p*GAL1-ACB1* grew with the same generation time (Figure 1A). However, when the 36-h galactose culture was diluted to OD 0.005 in 2% glucose medium and grown to late logarithmic phase at 30°C, Y700p*GAL1-ACB1* exhibited reduced growth rate and never reached wild-type OD after 24 h (Figure 1B). In galactose media, levels of Acb1p were increased ~10-fold in the Y700p*GAL1-ACB1* strain compared with wild-type cells (Figure 1, C and D). Acb1p levels in Y700p*GAL1-ACB1* declined very rapidly when cells were shifted to glucose medium (Figure 1C). Acb1p could no longer be detected by Northern blot or Western blot analysis, after growth under repressing glucose conditions for 24 h. If growth were continued, however, Acb1p reappeared at low levels after 36 h (Figure 1C). This is likely to be due to loss of repression by glucose in cultures that have past the diauxic shift. Cells used in all the following experiments were maintained on 2% galactose plates. When needed, a colony was picked and diluted to OD 0.005 and grown for 24 h in glucose medium, diluted to OD 0.1 in fresh glucose medium, and grown to the indicated optical density. Where indicated, the medium was supplemented with either 500 μM fatty acid/0.05% Brij58 or 25 μM PHS in the final culture subsequent to dilution of the overnight glucose culture. After each experiment, the absence of Acb1p was verified by Western blot analysis.

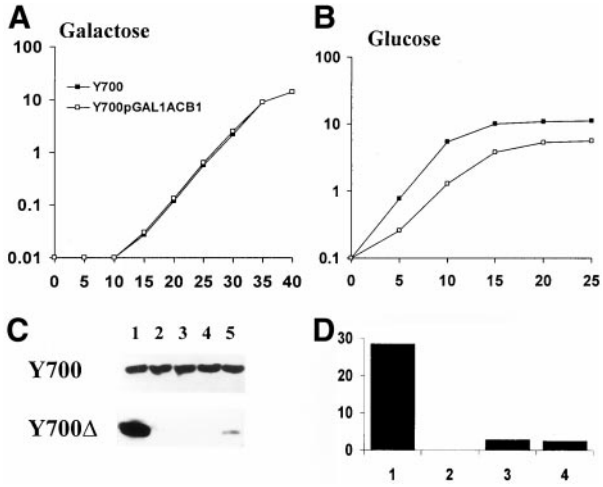

Figure 1. Growth curves of Y700 and Y700p*GAL1-ACB1* in YNB-galactose (A) and YNB-glucose (B) media. The growth was followed spectrophotometrically by measuring the cell density at 600 nm. (C) Acb1p levels in Y700 and Y700p*GAL1-ACB1* in cells grown in YNB-galactose for 48 h (lane 1) and in YNB-glucose for 24 h (lane 2), diluted into fresh YNB-glucose medium to OD 0.1 and grown to OD 0.2 (lane 3) and OD 0.5 (lane 4) and for 36 h (lane 5). (D) Quantitative data obtained by PhosphorImager analysis of a Northern blot of *ACB1* mRNA of Y700p*GAL1ACB1* and Y700 cells. Lane 1, Y700p*GAL1ACB1* grown in galactose; lane 2, Y700p*GAL1ACB1* grown in glucose; lane 3, Y700 grown in galactose; lane 4, Y700 grown in glucose. The *y*-axis is in arbitrary PhosphorImager units × 10^{-5}. For experimental details, see MATERIALS AND METHODS

Acb1p Is Required for Fatty Acid Elongation but Not for General Glycerolipid Synthesis

The level of total acyl-CoA in Y700p*GAL1-ACB1* cells grown under repressing conditions was identical to that of wild type. However, the relative content of stearoyl-CoA in Y700p*GAL1-ACB1* cells was increased 3.5-fold and that of unsaturated acyl-CoA was reduced 2- to 2.5-fold (Figure 2A). The relative content of C16:0-CoA remained unchanged. A similar increase in the relative amount of C18:0-CoA was previously observed in an adapted Y700*acb1*Δ strain (Schjerling *et al.*, 1996).

We have previously shown that overexpression of Acb1p in yeast results in a twofold increase in the total level of acyl-CoA esters (Knudsen *et al.* 1994). Remarkably, the 10-fold increased level of Acb1p in galactose-cultivated Y700p*GAL1-ACB1* cells did not affect fatty acid composition compared with wild type (Gaigg, Neergaard, Schneiter, Hansen, Færgeman, Jensen, Andersen, Friis, Sandhoff, Schrøder, and Knudsen, unpublished results). However, under repressing conditions dramatic changes in the fatty acid pattern were observed. The total content of fatty acids per OD_{600} unit was reduced to ~70% of wild type and the content of C26:0 fatty acid was reduced by ~70% (Figure 2B). The relative content of unsaturated fatty acids was increased by ~7%, and the ratio of C16:1 to C18:1 was increased by a factor of 1.6. A reduction in C26:0 synthesis was also observed in the adapted knock out strain in early logarithmic phase but disappeared when the cells reached stationary phase (Gaigg, Neergaard, Schneiter, Hansen,

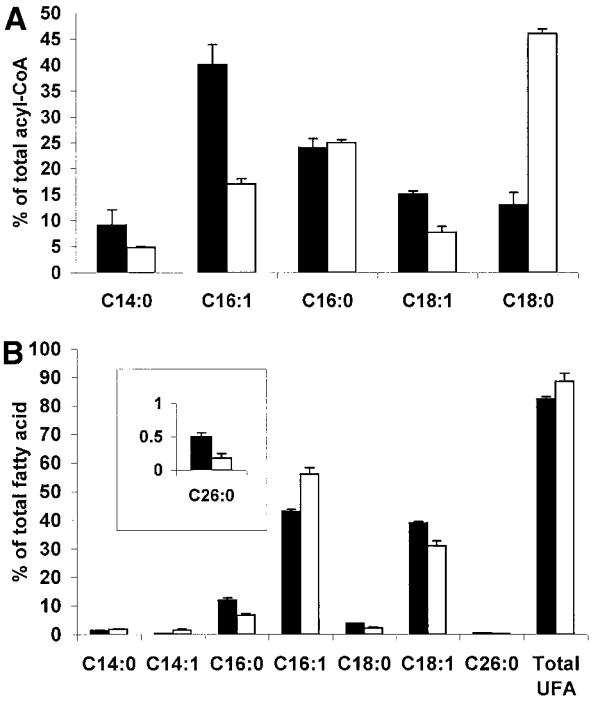

Figure 2. (A) Acyl-CoA composition of Y700 (black columns) and Y700p*GAL1ACB1* (open columns). The cells were grown in YNB-glucose for 24 h, diluted into fresh YNB-glucose medium to OD 0.05, grown to OD 0.2, harvested, and analyzed as described in MATERIALS AND METHODS. Values are means ± SEM of four independent experiments. (B) Total fatty acid composition of Y700 (black columns) and Y700p*GAL1-ACB1* (open columns). The cells were analyzed as described for A. Values are means ± SEM of six independent experiments and indicate total amounts of fatty acids/absorbance units of cells. UFA, unsaturated fatty acid (C14:1+C16:1+C18:1).

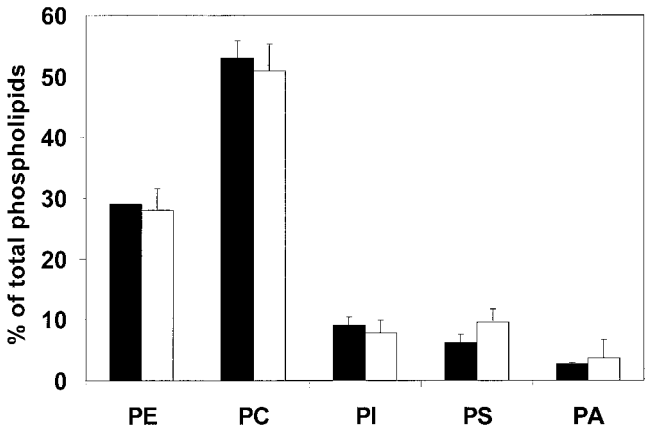

Figure 3. PL composition of Y700 (black columns) and Y700p*GAL1-ACB1* (open columns). Cells were labeled for six generations with 10 mCi [^{32}P]P_i/ml and analyzed as described in MATERIALS AND METHODS. Values are means ± SD of three independent experiments.

Færgeman, Jensen, Andersen, Friis, Sandhoff, Schrøder, and Knudsen, unpublished results). Fatty acid synthesis in yeast is terminated by the malonyl-CoA/palmitoyl-CoA transferase forming acyl-CoA as the end product, and the longest fatty acyl-CoA to be synthesized by this pathway is C18:0-CoA (Sumper and Trauble, 1973). The accumulation of fatty acid synthase end product C18:0-CoA and the simultaneously reduced elongation to C26:0 suggests that Acb1p is required for termination of fatty acid synthesis and transport of acyl-CoAs to the elongation systems.

When Y700 and Y700p*GAL1-ACB1* cells were grown to OD 0.2–0.5 in the presence or absence of 500 μM palmitic acid, the content of C26:0 was ~0.50% of the total fatty acids in Y700 and 0.22% in Y700p*GAL1-ACB1*. Despite a large increase in the level of C16-CoA upon supplementation with palmitic acid (Gaigg, Neergaard, Schneiter, Hansen, Færgeman, Jensen, Andersen, Friis, Sandhoff, Schrøder, and Knudsen, unpublished results), palmitic acid supplementation did not rescue C26:0 synthesis in Y700p*GAL1-ACB1*, indicating that elongation of both de novo synthesized and exogenously added C16:0 depend on Acb1p.

Because Acb1p binds long-chain acyl-CoA esters, loss of Acb1p function might be expected to affect glycerolipid synthesis. To examine PL synthesis in the Acb1p-depleted strain, cells were labeled with [^{32}P]P_i for six to seven generations, and the steady-state composition of PLs (Figure 3) and the turnover of the different PL classes were determined. The pattern of ^{32}P incorporation under steady-state labeling revealed that PL composition in the Y700p*GAL1-ACB1* was comparable to that of wild-type cells.

Calculation of turnover of individual PL classes from ^{32}P-pulse/chase experiments revealed that the half-life of phosphatidyl ethanolamine (PE), phosphatidyl serine (PS), and phosphatidyl inositol (PI) were very similar in the two strains 3.3 and 3.9, 2.8 and 2.8, and 5.3 and 5.1 h for the Y700 and Y700pGAL1-ACB1, respectively. Phosphatidyl choline (PC) turnover was slightly reduced in the Acbp1-depleted strain with a half-life of 5.6 h compared with 4.6 h in Y700. Synthesis of total and individual PL classes was also examined by [1-^{14}C]acetate pulse labeling. [1-^{14}C]acetate was added to exponentially growing cells (OD 0.5) cultured in glucose media. After 15 min, cells were harvested, and lipids were extracted and analyzed by TLC. Both strains incorporated similar amounts of [1-^{14}C]acetate. The TLC analysis revealed a pattern of incorporation into both neutral lipids and all major PL classes, which was identical in the two strains (Gaigg, Neergaard, Schneiter, Hansen, Færgeman, Jensen, Andersen, Friis, Sandhoff, Schrøder, and Knudsen, unpublished results). To our surprise, the results indicate that Acb1p is not required for general glycerolipid synthesis.

Acb1p Depletion Affects Expression of Genes Involved in Fatty Acid Desaturation But Not Elongation

To investigate the reason for reduced fatty acid elongation and increased fatty acid unsaturation in the Acb1p-depleted strain, we analyzed the expression levels of gene products involved in these processes. We and others have shown that *OLE1* mRNA was increased 3- and 5.5-fold in the adapted Y700*acb1*Δ and in JY001*acb1*Δ, respectively (Choi *et al.*, 1996; Schjerling *et al.*, 1996). The increased expression of *OLE1* was confirmed in glucose-grown Y700p*GAL1-ACB1* cells in

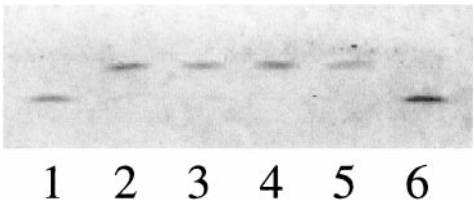

Figure 4. Determination of yeast ACBP ligand-binding specificity by isoelectric focusing. Yeast ACBP was incubated with threefold excess of different acyl-CoAs and focused on an isoelectric focusing gel. Binding of acyl-CoA is identified by band shift. Lane 1, without ligand; lane 2, C16:0-CoA; lane 3, C18:0-CoA; lane 4, C20:0-CoA; lane 5, C22:0-CoA; lane 6, C24:0-CoA.

which the level of *OLE1* mRNA was increased fivefold (Gaigg, Neergaard, Schneiter, Hansen, Færgeman, Jensen, Andersen, Friis, Sandhoff, Schrøder, and Knudsen, unpublished results). The higher proportion of unsaturated fatty acids in Y700p*GAL1-ACB1* might therefore be caused by the increase in Δ-9-desaturase activity. In the yeast *S. cerevisiae*, three membrane-bound enzymes, Elo1/2/3p, catalyze elongation of fatty acids. Elo1p is involved in elongation of C14:0-fatty acid to C16:0 (Toke and Martin, 1996). Elo2/3p acts downstream of Elo1p and catalyzes the elongation of fatty acids to C24:0 and C26:0, respectively (Oh *et al.*, 1997). The mRNA levels of all three fatty acid elongation enzymes were unchanged in Y700p*GAL1-ACB1* cells grown under glucose-repressing conditions (Gaigg, Neergaard, Schneiter, Hansen, Færgeman, Jensen, Andersen, Friis, Sandhoff, Schrøder, and Knudsen, unpublished results). The requirement of Acb1p in fatty acid elongation could be at three different levels. Transport of de novo synthesized acyl-CoA esters from the fatty acid syntase to the elongases, shuttling of acyl-CoA intermediates between the individual elongases or removal of the final acyl-CoA product. Acb1p has been shown to bind C16:0-CoA with a KD of 2.3 nM (Fulceri *et al.*, 1997). Because binding of negatively charged acyl-CoA to Acb1p changes the isoelectric point, we used isoelectric focusing to determine the relative binding affinities of long-chain and very long-chain acyl-CoA esters to yeast Acb1p. From Figure 4 it can be seen that C16:0-, C18:0-, and C20:0-CoA esters shift the isoelectric point of Acb1p, whereas C22:0-CoA is less efficient. In contrast, C24:0-CoA is unable to bind to Acb1p and does not shift its isoelectric point. It is therefore unlikely that Acb1p is required for either shuttling of VLCFA-CoAs between elongases or removal of the elongation product. The above results rather suggest that Acb1p is involved in transport of long chain acyl-CoA to the elongases.

Depletion of Acb1p Affects Sphingolipid Synthesis

Inositol-phosphoceramide (IPC), mannose-IPC (MIPC), and mannose-(inositol-P)$_2$-ceramide (M(IP)$_2$C) are the three major classes of sphingolipids in *S. cerevisiae*. Sphingolipids, which previously have been reported to comprise ~7–8% of the plasma membrane mass and 30% of the plasma membrane lipids, respectively (Patton and Lester, 1991, 1992), contain almost exclusively C26:0 and hydroxy-C26:0 fatty acids in their hydrophobic ceramide moiety (Lester *et al.*, 1993). Because of the pronounced reduction in the level of

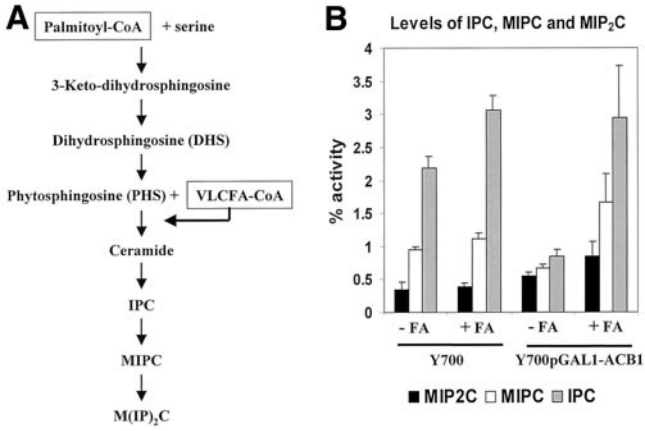

Figure 5. Sphingolipid synthesis. (A) General outline of the sphingolipid synthesis pathway in *S. cerevisiae*. (B) Cells grown in glucose for 24 h were labeled with [^{3}H]*myo*-inositol to steady state in the presence (+) or absence (−) of fatty acid (FA; 500 μM C16:0/0.05% Brij), and levels of the three major classes of sphingolipids were determined by scintillation counting and HPTLC. Levels are given as percentages ± SEM of total lipid − extractable [^{3}H]*myo*-inositol activity (n = 3–6).

C26:0 fatty acid, we examined whether depletion of Acb1p affects the synthesis of complex lipids.

Therefore, Y700 and Y700p*GAL1-ACB1* cells were grown for 6–7 h (steady state) in the presence of radiolabeled [^{3}H]*myo*-inositol in a medium containing 11 μM inositol.

Radiolabeling of total lipids in Y700p*GAL1-ACB1* was only 50% of the labeling in Y700. In wild-type cells and in Y700p*GAL1-ACB1* cells, 3.5 and 2%of the total lipid-extractable radioactivity, respectively, was found in sphingolipids (Figure 5B). Remarkably, the low [^{3}H]*myo*-inositol radioac-

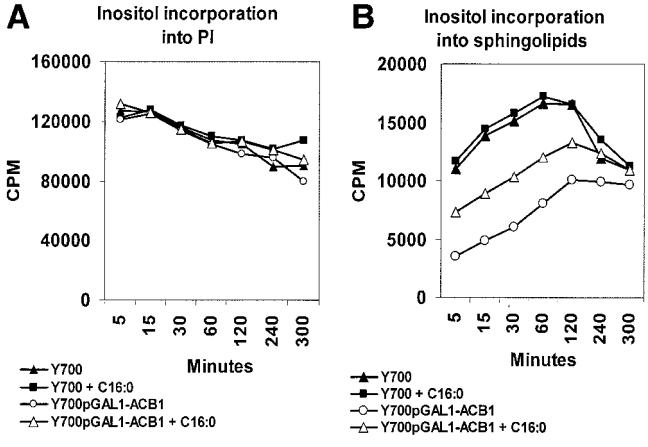

Figure 6. Incorporation of [^{3}H]*myo*-inositol into PI and sphingolipids. (A) Cells were pulse labeled for 15 min and chased for 5 h. Cells were harvested at the indicated times, lipids were extracted, and total [^{3}H]*myo*-inositol incorporation was determined by scintillation counting. (B) After mild alkaline hydrolysis and re-extraction, the amount of [^{3}H]*myo*-inositol in the sphingolipids was determined. Data are means (±SEM) of three independent determinations.

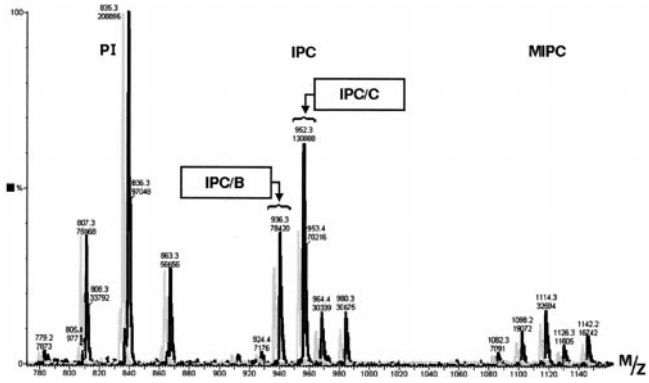

Figure 7. Mass spectrometric determination of PI, IPC, and MIPC in plasma membrane lipids from Y700 (gray) and Y700p*GAL1-ACB1* (black). IPC/C contains PHS C18 and a C26OH fatty acid; IPC/B (or IPC/B′) contains phytospingosine C18 and a C26 fatty acid or dihydrosphingosine C18 and a C26OH fatty acid.

tivity incorporated into sphingolipids in Y700p*GAL1-ACB1* was solely due to a reduced incorporation into IPC and MIPC. Incorporation into $M(IP)_2C$ was slightly increased in Y700p*GAL1-ACB1* cells compared with wild type.

Supplementation with 500 μM palmitic acid/0.05% Brij 58 in the incubation medium, of the final culture, restored the relative incorporation of [^{3}H]inositol into individual inositol-sphingolipid species (Figure 5B) and increased total [^{3}H]inositol incorporation into sphingolipids.

To examine the reduction in inositol incorporation in the Acb1p-depleted strain in more detail, Y700p*GAL1-ACB1* and Y700 cells were pulse labeled in inositol-free medium at high cell density (OD 10) to ensure momentarily and complete uptake of [^{3}H]inositol. After pulse labeling the cells were chased by addition of a large volume of fresh medium containing unlabeled inositol. No difference was observed in [^{3}H]*myo*-inositol incorporation in PI during the pulse or in PI turnover during the chase, between wild type and Y700p*GAL1-ACB1* in either the absence or presence of palmitic acid (Figure 6A). These data thus confirm the results obtained by [^{32}P]- and [1-^{14}C]acetate labeling and are consistent with the fact that depletion of Acb1p does not affect the synthesis of glycerophospholipids. However, Y700p*GAL1-ACB1* displayed a strongly reduced initial incorporation of [^{3}H]*myo*-inositol into sphingolipids (30% of wild type), and transfer of [^{3}H]inositol from PI to sphingolipids during chase was delayed. The reduced slope of the descending part of the sphingolipid labeling curves (Figure 6B) suggests that the Y700p*GAL1-ACB1* strain also exhibits delayed turnover of sphingolipids compared with wild-type cells. Again, the steady-state labeling medium contained inositol, and the reduction in sphingolipid labeling was solely due to a reduction in IPC and MIPC labeling, whereas [^{3}H]*myo*-inositol incorporation into $M(IP)_2C$ was unchanged (Gaigg, Neergaard, Schneiter, Hansen, Færgeman, Jensen, Andersen, Friis, Sandhoff, Schrøder, and Knudsen, unpublished results).

Table 1. Mass spectroscopic analysis of the relative levels of LPs in individual phospholipid classes in plasma membranes isolated from wild type or cells depleted of Acb1

	% Lyso of total		
Lipid	Wild type	pGAL-ACB1	Ratio
PA	16.3	28.0	1.71
PC	6.4	7.3	1.14
PE	8.1	9.9	1.22
PS	4.0	7.7	1.93
PI	6.3	13.6	2.16

Values shown are percentages of lysolipid of total phospholipids in each class.

Table 2. Mass spectroscopic analysis of the relative levels of LPA and PA species of plasma membranes isolated from wild type or cells depleted of Acb1p

m/z	Species	Wild type	pGAL-ACB1
407	16;1	10.9	4.8
409	16;0	2.4	2.1
435	18;1	14.6	9.3
643	32;2	14.3	15.6
645	32;1	9.2	7.3
671	34;0	27.4	42.2
673	34;1	21.1	18.7

For experimental detail, see the MATERIALS AND METHOD section.

Plasma Membrane IPC and MIPC Levels Are Increased in the Acb1p-depleted Strain

If reduced [^{3}H]*myo*-inositol incorporation into IPC was caused by decreased synthesis of this lipid, it would be expected that Y700p*GAL1-ACB1* contained less inositol-sphingolipid in the plasma membrane. Mass spectrometric analysis of plasma membrane phospho- and sphingolipid species revealed that the level and pattern of individual PI species were comparable to wild type in the Acb1p-depleted strain (Figure 7). Surprisingly, however, this analysis revealed that the relative levels of IPC and MIPC were 25–40% increased in Y700p*GAL1-ACB1* compared with Y700. The

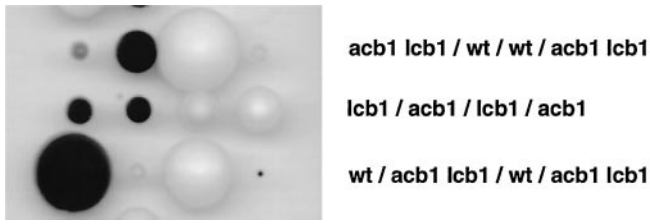

Figure 8. Tetrad analysis of a cross between Y700pGAL1-ACB1 and lcb1–100. Genotype of the spores is indicated to the right. Note the reduced growth on glucose of p*GAL1-ACB1* lcb1–100 double mutants after growth at 30°C for 6 d.

pattern of individual IPC and MIPC species, however, was comparable in the two strains. The two major species were IPC/C containing PHS with 18 carbons and a C26OH fatty acid and IPC/B or IPC/B′ containing phytospingosine C18 and a C26 fatty acid or dihydrosphingosine C18 and a C26OH fatty acid, respectively.

It is interesting to note that the relative level of IPC and MIPC is increased, although the incorporation of [^{3}H]*myo*-inositol into these two species is strongly reduced in the Acb1p-depleted strain. This may indicate that the decreased labeling of these two lipids is due to a decreased turnover. This hypothesis is supported by the fact that sphingolipid turnover in Y700p*GAL1-ACB1* is decreased compared with wild type (Figure 6B).

The mass spectroscopic analysis also revealed that the relative levels of LPA, lysophosphatidylserine and lysophosphatidylinositol were significantly increased in Y700pGAL1-ACB1 compared with Y700 (Table 1), indicating a lack of acyl-CoA for acylation of lysophospholipids in remodeling of PLs at the plasma membrane.

The increased level of LPA was caused by an increase in the unsaturated LPA species only (Table 2) and was accompanied by a large decrease in the content of C16:1/C18:1-phosphatidic acid (PA). This may indicate that Acb1p is required for delivery of C16:1- or C18:1-acyl-CoA for synthesis of this particular PA species in the plasma membrane.

Genetic Interaction between lcb1 and GAL1-ACB1

Both acyl-CoA entry points in the sphingolipid synthesis pathway could potentially be affected by depletion of Acb1p (Figure 5A): Delivery of palmitoyl-CoA to Lcb1p/Lcb2p, which catalyzes the initial step of PHS synthesis, could be reduced. Alternatively, reduced delivery of VLCF-acyl-CoAs to the ceramide synthase could be the step affected.

Addition of 500 μM palmitic acid/0.05% Brij 58 to the medium used for growing Y700p*GAL1-ACB1* for pulse labeling increased [^{3}H]*myo*-inositol incorporation into sphingolipids to ~70% of wild-type level by increasing incorporation into IPC and MIPC (Figure 5B) but never restored sphingolipid synthesis completely. Addition of PHS did not affect total [^{3}H]*myo*-inositol incorporation into sphingolipids or the incorporation pattern into individual sphingolipid species in Y700p*GAL1-ACB1*.

Tetrad analysis of a diploid strain made by mating Y700p*GAL1-ACB1* and the temperature-sensitive lcb1 mutant (*lcb1–100;* Sutterlin *et al.*, 1997) showed that the *acb1 lcb1* double mutant spores grew extremely slowly at permissive temperature (Figure 8). This indicates that PHS synthesis is partly reduced in Y700p*GAL1-ACB1,* although it is not rate limiting for sphingolipid synthesis. The reduced PHS synthesis becomes visible only when both mutations occur at the same time, consistent with the notion that both mutations affect the same pathway, namely, synthesis of PHS.

The altered pattern of [^{3}H]*myo*-inositol incorporation into sphingolipids in Y700p*GAL1-ACB1* is different from what would be expected if sphingolipid synthesis was reduced because of lack of VLCFA synthesis (Oh *et al.*, 1997). No genetic interaction could be observed by crossing elongase mutants with *acb1*Δ (Gaigg, Neergaard, Schneiter, Hansen, Færgeman, Jensen, Andersen, Friis, Sandhoff, Schrøder, and Knudsen, unpublished results).

The [^{3}H]*myo*-inositol incorporation pattern observed in the Acb1p-depleted strain resembled the pattern observed

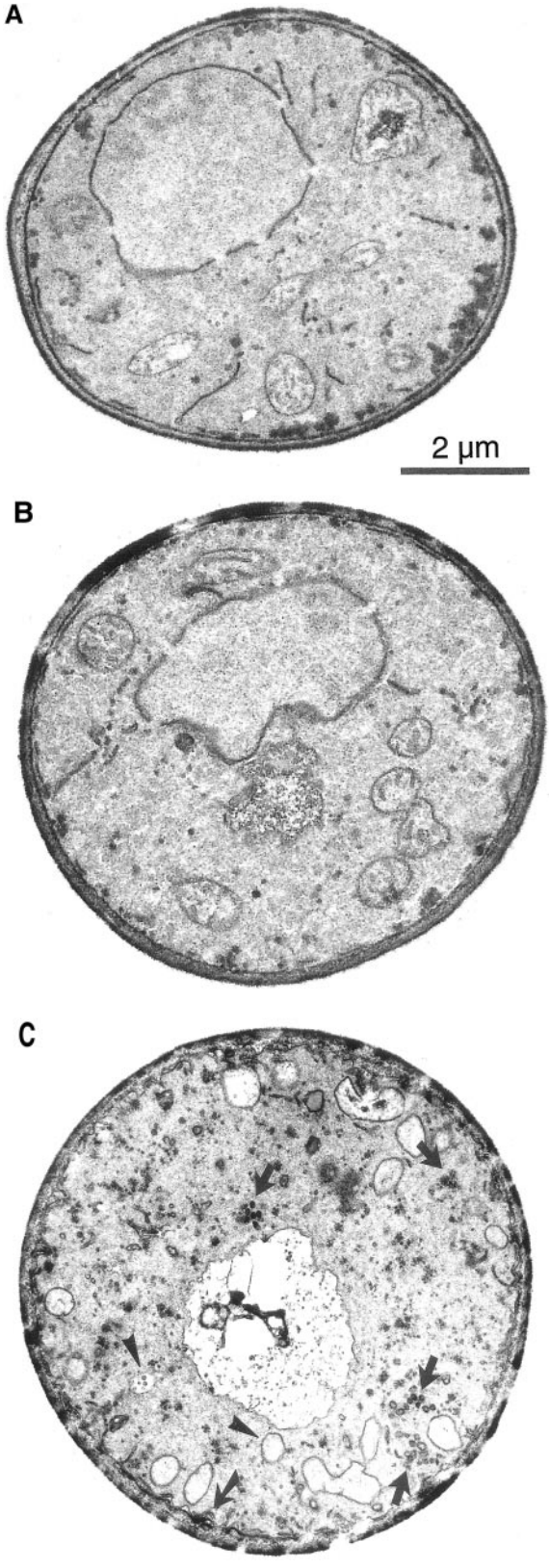

Figure 9.

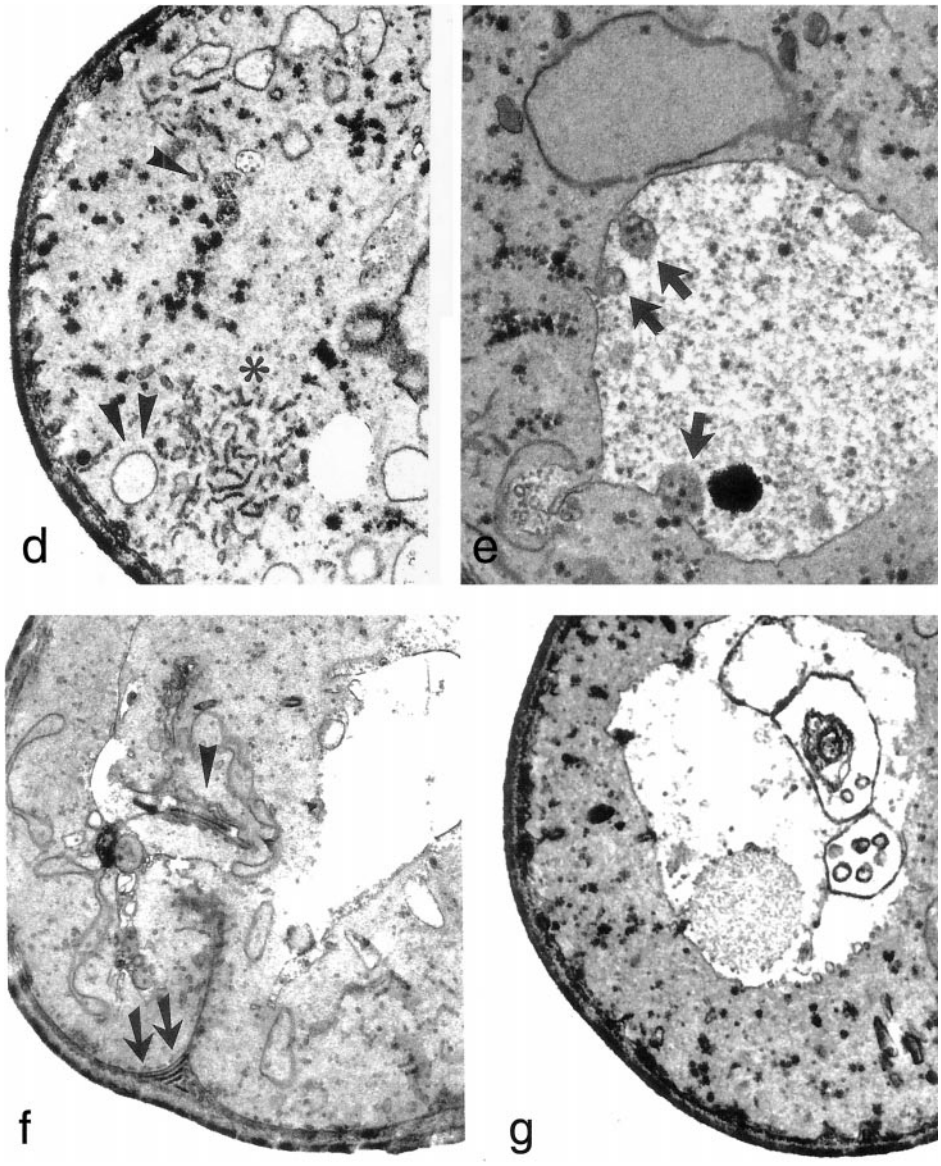

Figure 9 (cont).

when sphingolipid synthesis is abrogated because of inhibition of Golgi function by brefeldin A (BFA; Hechtberger and Daum, 1995). This fact may indicate that the altered sphingolipid synthesis in the Acb1p-depleted strain is due to impaired vesicular trafficking or membrane organization. To investigate this phenomenon further, we analyzed the organelle and membrane structure by electron microscopy.

Cells Depleted of Acb1p Display Aberrant Membrane Profiles

The level of Acb1p in Y700p*GAL1-ACB1* cells grown in galactose medium is 8- to 10-fold higher than that of wild type (Figure 1). This increased level of Acb1p in Y700p*GAL1-ACB1* did not affect membrane morphology of this strain compared with wild type grown on galactose (Figure 9, a and b). In contrast, cells depleted of Acb1p accumulated a large number of variably sized vesicles and granules (Figure 9c, arrows), and many cells also showed multilayer plasma membrane domains (Figure 9, c and f, fancy arrows). A large number of cells contained what could be interpreted as autophagocytotic like bodies (Figure 9, c and d, arrowheads) and randomly organized dense membrane areas (Figure 9d, star). Vacuolar inclusions of vesicles containing autophagocytotic like bodies were observed frequently (Figure 9e, arrows). Some cells exhibiting multilayer plasma membrane domains also showed large invaginations of the plasma membrane and accumulation of membrane material in the cytosol (Figure 9f, arrowhead). In some cases,

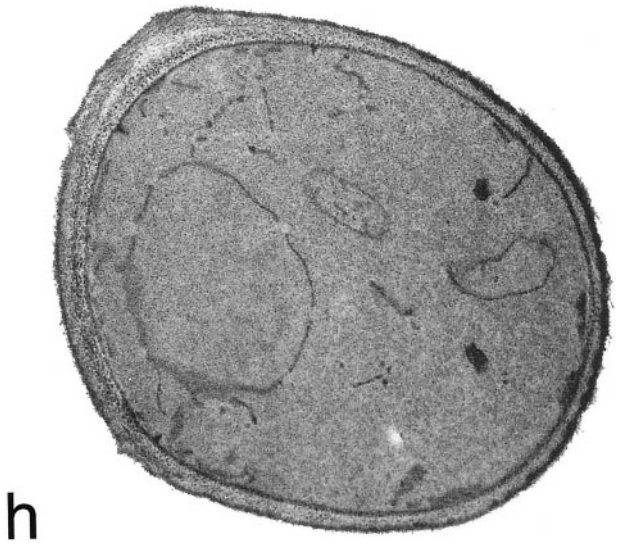

Figure 9 (cont). Acb1p-depleted cells exhibit severe membrane alterations. Wild-type and Acb1p-depleted cells were grown in galactose (a and b, respectively) and in glucose media (h and c–g, respectively) and were prepared for electron microscopy. When grown on glucose, Acb1p-depleted cells accumulate vesicles of variable sizes (c, arrow), autophagocytotic bodies (c and d, arrowheads), randomly organized dense membrane areas (d, star), vacuolar inclusions of vesicles containing autophagocytotic like bodies (e, arrows), large invaginations of plasma membrane and accumulation of membrane material in the cytosol (f, arrowhead), and accumulation of membrane material in the vacuole (g).

we observed a large amount of membrane material within the vacuole, which could result from engulfment of the plasma membrane invaginations (Figure 9, g and f). None of these structures were observed in wild-type cells grown under identical conditions (Figure 9h). These results indicate very strongly that depletion of Acb1p affects vesicular trafficking, membrane biogenesis, and the structure of the plasma membrane.

Y700pGAL1-ACB1 Exhibits Altered Cell Wall and Plasma Membrane Properties

A defect in vesicular trafficking and an altered plasma membrane structure and lipid composition is likely to affect the integrity of the yeast cell wall and transport across the plasma membrane. In yeast, inositol is taken up by two transporters, *ITR1* and *ITR2*, of which one (*ITR1*) is repressed by inositol in the medium (Nikawa *et al.*, 1993). We therefore investigated inositol uptake in cells pregrown in either the presence of inositol in the medium. Inositol uptake was strongly reduced in Y700p*GAL1-ACB1* independently of the presence of inositol in the medium during the culturing (Figure 10A). These results differ from what would be expected from the [^{3}H]*myo*-inositol pulse labeling of inositol-containing lipids (Figure 6B). In this experiment, the labeling of PI was similar in Y700 and Y700p*GAL1-ACB1.* This difference is most likely caused by the high cell density (10 OD unit/ml) present in the pulse-chase experiment compared with the uptake experiment (1 OD unit/ml), which

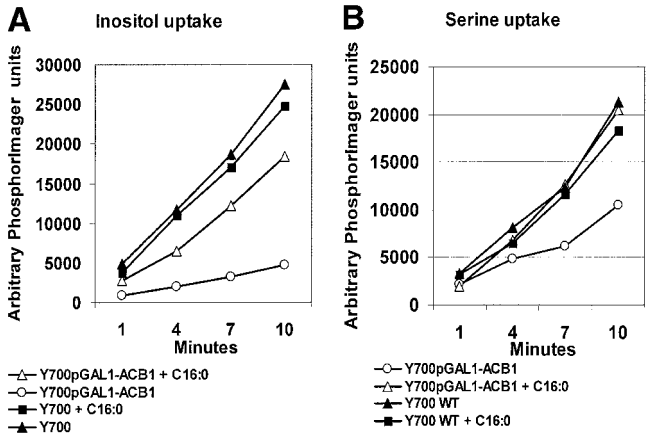

Figure 10. Uptake of radiolabeled inositol and serine from the medium. Y700p*GAL1-ACB1* and Y700 were grown to early log phase in the presence of inositol, harvested, and resuspended in PBS to an OD of 1.0. (For details, see MATERIALS AND METHODS). After addition of radiolabeled inositol (A) or serine (B), uptake was stopped by transferring the cells to ice-cold PBS containing excess unlabeled inositol or serine, at the times indicated. Cells were collected by vacuum filtration, the filter paper was dried (for details, see MATERIALS AND METHODS), and the ^{3}H activity of each cell spot was quantified by phosphorimaging.

ensures complete uptake of the very small amount of inositol added during the 5-min pulse. The fact that uptake of [^{3}H]serine was also strongly reduced in Y700p*GAL1-ACB1* (Figure 10B) indicates that uptake of nutrients from the medium by active transport is a general defect of cells depleted of Acb1p. Addition of 500 μM palmitic acid to the medium as described above partly restored inositol uptake and restored serine uptake completely (Figure 10). In addition to the decreased inositol uptake in cells depleted of Acb1p, these cells also exhibited an Opi$^-$ phenotype and excreted inositol (Gaigg, Neergaard, Schneiter, Hansen, Færgeman, Jensen, Andersen, Friis, Sandhoff, Schrøder, and Knudsen, unpublished results). The altered membrane and cell wall properties of cells depleted of Acb1p were further explored by testing their sensitivity to various detergents. When grown in glucose medium in the presence of different concentrations of the detergent Brij58, Y700p*GAL1-ACB1* was severely inhibited by increasing concentrations of Brij58 in the medium, whereas wild-type cells were only slightly affected (Figure 11A). Addition of fatty acids to the medium restored growth of Y700p*GAL1-ACB1* in the presence of all concentrations of Brij58 (Figure 11A).

Susceptibility of *S. cerevisiae* to lysis by glucanase-protease mixtures is a qualitative assay to test the state of cell walls (Ovalle *et al.*, 1998). Cells depleted of Acb1p were hypersensitive to Zymolyase treatment and displayed a total lack of lag time characteristically observed in wild-type cells (Figure 11B).

DISCUSSION

The presented results suggest a specific role for Acb1p in synthesis of VLCFA and membrane lipid turnover and trafficking. The composition of the long-chain acyl-CoA in the

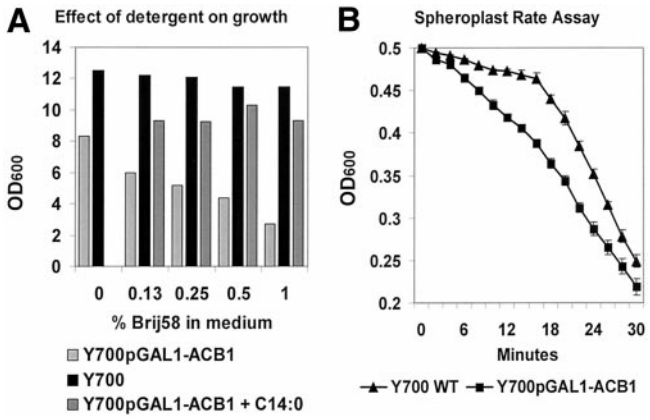

Figure 11. Test of cell envelope integrity. (A) Y700p*GAL1-ACB1* and Y700 were diluted to OD 0.1 and grown in the presence of different concentrations of the detergent Brij58. After 16 h the OD_{600} of each culture was determined. (B) Y700p*GAL1-ACB1* and Y700 were resuspended to OD 0.5 and treated with Zymolyase while the optical density was monitored. Data shown ± SEM (n = 3).

Acb1p-depleted strain was dramatically changed without any change in pool size. The relative amount of C18:0-acyl-CoA is increased 3.5-fold with a compensatory decrease in the other acyl-CoAs. Similar changes in acyl-CoA composition have previously been reported in an adapted *ACB1*-deleted strain; however, this strain also exhibited a 2.5-fold increase in pool size, which could be part of the adaptation mechanism (Schjerling *et al.*, 1996). It is interesting that the acyl-chain composition of the acyl-CoA pool is very different from that of the total fatty acid pool in both Y700p*GAL1-ACB1* and Y700. This indicates that the total fatty acid composition is not determined by the availability of acyl-CoAs in the cellular acyl-CoA pool or that the acyl-CoA esters for glycerolipid synthesis originate from a unique and different pool. Alternatively, the acyl-CoA transferases are saturated with the preferred substrates. This indicates that Acb1p is not required for all aspects of lipid synthesis but rather for specialized functions. The identical steady-state ^{32}P labeling and turnover of ^{32}P-labeled PL species by wild type and Y700p*GAL1-ACB1* indicate that Acb1p is not required for general glycerolipid synthesis. This is further supported by the identical [^{3}H]*myo*-inositiol incorporation into PI and the identical turnover of this lipid in the two strains.

Y700p*GAL1-ACB1* contained, in contrast to the previous reported Acb1p deletion strain, increased levels of unsaturated fatty acids in total lipids. This observation combined with the fact that general glycerolipid synthesis is not affected by deletion of Acb1p indicate that Ole1p can obtain its substrate by a different route than from Acb1p, perhaps by a direct interaction with FAS. The increased level of *OLE1* mRNA might, therefore, explain the increased level of unsaturated fatty acid. Direct interaction of enzymes with fatty acid synthetase has previously been shown for thioesterase II in the termination of medium chain fatty acid synthesis in rodents (Knudsen, 1979; Mikkelsen *et al.*, 1987).

The most dramatic change in fatty acid composition was the strong reduction in C26:0 levels accompanied by a shift to shorter fatty acids, indicating a direct or indirect involvement of Acb1p in VLCFA synthesis. The fact that Acb1p does not bind VLCFA-CoAs (Figure 4) excludes the possibility that the protein is involved in transfer of VLCFA-CoA between Elo2p and Elo3p and in product removal from the elongases. This and the accumulation of the FAS end product (C18:0-CoA) suggest that Acb1p is involved in transport of de novo synthesized acyl-CoA from FAS to the elongase. Furthermore, deletion of *ACB1* did not affect *ELO2* and *ELO3* mRNA levels (Gaigg, Neergaard, Schneiter, Hansen, Færgeman, Jensen, Andersen, Friis, Sandhoff, Schrøder, and Knudsen, unpublished results), which suggests that the observed reduction in VLCFA synthesis is not caused by a reduced activity of Elo2p and Elo3p.

The observation that depletion of Acb1p in the temperature-sensitive mutant of *ACC1, mtr7-1* (Schneiter *et al.*, 1996), which exhibits reduced synthesis of C26:0 fatty acid already at permissive temperature, results in lethality (Gaigg, Neergaard, Schneiter, Hansen, Færgeman, Jensen, Andersen, Friis, Sandhoff, Schrøder, and Knudsen, unpublished results) indicates that both proteins are active in the same pathway. The reduced levels of C26:0 fatty acid in Y700p*GAL1-ACB1* cannot be rescued by supplying cells with exogenous fatty acids (C16:0), indicating that Acb1p is required for elongation of both newly synthesized acyl-CoAs from FAS and exogenous added palmitic acid (Gaigg, Neergaard, Schneiter, Hansen, Færgeman, Jensen, Andersen, Friis, Sandhoff, Schrøder, and Knudsen, unpublished results). The ability of Y700p*GAL1-ACB1* to synthesize low levels of C26:0 fatty acid suggests that there are other pathways by which acyl-CoAs are transported to the elongating enzymes than the Acb1p-dependent pathway. Alternatively, Acb1p is not required for VLCFA synthesis, leading to the suggestion that reduced synthesis of VLCFA is secondary to a decrease in synthesis of sphingolipids.

C26 fatty acids are mainly found in the ceramide moiety of sphingolipids, and reduced synthesis and turnover of ceramide and sphingolipid could therefore increase the pool of VLCFA-CoAs available and feedback inhibit further VLCFA synthesis. Sphingolipid synthesis could also be limited by the lack of palmitoyl-CoA for the initial step of PHS synthesis, which is also required for ceramide synthesis. This is unlikely to be the case because addition of PHS did not stimulate [^{3}H]*myo*-inositol incorporation into sphingolipids during pulse labeling with [^{3}H]*myo*-inositol. However, the retarded growth of the acb1 lcb1 double mutant at permissive temperature indicated a common defect in long chain base synthesis. Addition of fatty acids (C16:0) to the medium, however, partly re-established sphingolipid synthesis and partly restored the ratios of the three sphingolipid species in Y700p*GAL1-ACB1* (Figures 5B and 6B). It is tempting to suggest that the stimulation of sphingolipid synthesis by C16:0 is achieved by an increased synthesis of C26 fatty acids. However, the fact that addition of C16:0 does not restore C26:0 fatty acid levels, yet rescues sphingolipid synthesis, makes it unlikely that it is a lack of VLCFAs that is rate limiting for sphingolipid synthesis.

Using well defined temperature-sensitive secretion mutants, Puoti *et al.* (1991) demonstrated that the biosynthesis of MIPC, $M(IP)_2C$, and some IPC species is dependent on genes required for vesicular transport of proteins from endoplasmic reticulum (ER) to the Golgi apparatus.

Glycosylphosphatidylinositol (GPI)-anchored proteins are inserted into ceramide/sphingolipid rafts already in the ER

(Bagnat *et al.*, 2000), suggesting that GPI-anchored proteins and sphingolipids are cotransported from the ER to the plasma membrane. Strains carrying mutations in genes encoding proteins responsible for addition of GPI anchors to proteins also exhibit strongly reduced sphingolipid synthesis (Leidich *et al.*, 1994; Schonbachler *et al.*, 1995). It has been shown that serine-palmitoyl transferase (Lcb1p/Lcb2p) activity was reduced by 80% in these strains. The authors suggested that the lack of addition of GPI anchors prevented cotransport of sphingolipids and the GPI-anchored proteins out of the ER, leading to accumulation of ceramide or IPC in the ER and repression of Lcb1p and/or Lcb2p (Schonbachler *et al.*, 1995).

BFA disassembles the Golgi apparatus and thereby blocks transport between the ER and Golgi. Treatment of yeast with BFA caused growth inhibition but did not affect incorporation of [^{3}H]inositol into total lipids (sphingolipids and PI; Hechtberger and Daum, 1995). The amount of label incorporated into IPC and MIPC was dramatically reduced, whereas the incorporation into $M(IP)_2C$ was unaffected, which we also observed in Y700p*GAL1-ACB1* in the present study. The authors suggested that BFA disturbed the transport-linked metabolic conversion of IPC to MIPC and that the Golgi synthesizes or contains sufficient unlabeled MIPC to support continued [^{3}H]*myo*-inositol incorporation into $M(IP)_2C$.

The facts that sphingolipid synthesis is tightly coupled to vesicular trafficking and that [^{3}H]*myo*-inositol labeling of Y700p*GAL1-ACB1* matches the labeling pattern in BFA-treated cells indicate that the reduced sphingolipid synthesis in the Acb1p-depleted strain is due to a decreased IPC turnover caused by perturbed vesicular trafficking. This assumption is supported by the facts that PHS did not stimulate [^{3}H]*myo*-inositol incorporation into sphingolipids and that fatty acids did not stimulate C26:0 synthesis. Furthermore, when the supply of VLCFA-CoAs for ceramide synthesis is blocked by mutation in either *ELO2* or *ELO3,* a general reduction in the synthesis of all sphingolipid species is observed (Oh *et al.*, 1997) and not IPC and MIPC alone, as seen in the Acb1p-depleted strain.

The relative level of IPC and MIPC in the plasma membrane is increased in the Acb1p-depleted strain, although the incorporation of [^{3}H]*myo*-inositol into these two species is strongly reduced. This indicates that the reduced synthesis observed by [^{3}H]*myo*-inositol labeling is caused by a reduced turnover of these lipids.

This hypothesis is supported by the reduced sphingolipid labeling and turn over in Y700p*GAL1-ACB1* compared with wild type (Figure 6B). The accumulation of IPC and MIPC in the plasma membrane could indicate that trafficking of sphingolipids from the plasma membrane to the cell interior is abrogated.

This hypothesis is strongly supported by the observed accumulation of large amounts of differently sized vesicles, multilayer plasma membrane domains, autophagosomes or autophagocytotic/endosome-like bodies, and membrane fragment-containing vacuoles in Y700p*GAL1-ACB1*. These abnormalities indicate that Y700pGAL1-ACB1 has an abnormal membrane trafficking in general.

The electron microscopy studies suggest an increased autophagocytotic activity in Y700p*GAL1-ACB1,* presumably to cope with the accumulation of membrane material in the form of vesicles and abnormal plasma membrane structures. The above results strongly indicate that Acb1p plays an important role in transport-mediated lipid synthesis. The observation that Y700p *GAL1-ACB1* also shows delayed maturation of a number of proteins, including amino peptidase 1 (Gaigg, Neergaard, Schneiter, Hansen, Færgeman, Jensen, Andersen, Friis, Sandhoff, Schrøder, and Knudsen, unpublished data), indicates that the role of Acb1p in trafficking is not limited to lipid/membrane trafficking at the plasma membrane level.

A requirement for long-chain acyl-CoA esters for budding and fusion of vesicles was reported earlier (Glick and Rothman, 1987; Pfanner *et al.*, 1989, 1990; Rothman and Wieland, 1996). The addition of a thioether analogue of palmitoyl-CoA blocked both budding from ER and fusion of ER-derived vesicles with Golgi membranes (Pfanner *et al.*, 1989). Budding of synaptic-like microvesicles and Golgi vesicles has recently been shown to require acyl-CoA for conversion of LPA to PA, catalyzed by the lysophosphatidic acid acyltransferases endophilin and CtBP/BARS, respectively (Schmidt *et al.*, 1999; Weigert *et al.*, 1999).

The fact that both the plasma membrane level of LPA is almost doubled and that the relative content of C16:0/C18:1-PA are significantly reduced in Y700p*GAL1-ACB1* indicate that similar mechanisms may exist in yeast and that they depend on Acb1p.

ACBP/Acb1p binds acyl-CoA esters with very high affinity and is always expressed at very high levels in secretory tissues of higher eukaryotes (Færgeman and Knudsen, 1997). This fact combined with the observed defects in membrane trafficking in Y700p*GAL1-ACB1* suggest a role for Acb1p in delivery of acyl-CoA in these pathways.

Supplementation of palmitic acid can partly restore the transport phenotype, indicating that reduced availability of acyl-CoA for budding and fusion in Y700p*GAL1-ACB1* can be overcome by acyl-CoA synthesized from exogenous fatty acids by the fatty acid-activating enzymes such as Faa1p and Faa4p.

In summary, the present results strongly indicate that Acb1p is not required for general glycerolipid synthesis but is necessary for normal synthesis of VLCFAs and that Acb1p plays an important role in transport-mediated lipid synthesis and membrane trafficking.

ACKNOWLEDGMENTS

We would like to thank the Center for Interaction, Structure, Function and Engineering of Macromolecules and The Carlsberg Foundation for financial support.

REFERENCES

Bagnat, M., Karanen, S., Shevchenko, A., and Simons, K. (2000) Lipid rafts function in biosyntetic delivery of proteins to the cell surface in yeast. Proc. Natl. Acad. Sci. USA *97*, 3254–3259.

Borsting, C., Hummel, R., Schultz, E.R., Rose, T.M., Pedersen, M.B., Knudsen, J., and Kristiansen, K. (1997). *Saccharomyces carlsbergensis* contains two functional genes encoding the acyl-CoA binding protein, one similar to the ACB1 gene from *S. cerevisiae* and one identical to the ACB1 gene from *S. monacensis.* Yeast *13*, 1409–1421.

Choi, J.Y., Stukey, J., Hwang, S.Y., and Martin, C.E. (1996). Regulatory elements that control transcription activation and unsaturated

fatty acid-mediated repression of the *Saccharomyces cerevisiae* OLE1 gene. J. Biol. Chem. *271*, 3581–3589.

Færgeman, N.J., and Knudsen, J. (1997). Role of long-chain fatty acyl-CoA esters in the regulation of metabolism and in cell signaling. Biochem. J. *323*, 1–12.

Færgeman, N.J., Sigurskjold, B.W., Kragelund, B.B., Andersen, K.V., and Knudsen, J. (1996). Thermodynamics of ligand binding to acyl-coenzyme A binding protein studied by titration calorimetry. Biochemistry *35*, 14118–14126.

Fulceri, R., Knudsen, J., Giunti, R., Volpe, P., Nori, A., and Benedetti, A. (1997). Fatty acyl-CoA-acyl-CoA-binding protein complexes activate the Ca^{2+} release channel of skeletal muscle sarcoplasmic reticulum. Biochem. J. *325*, 423–428.

Geisbrecht, B.V., Zhang, D., Schulz, H., and Gould, S.J. (1999). Characterization of PECI, a novel monofunctional Delta(3), Delta(2)-enoyl-CoA isomerase of mammalian peroxisomes. J. Biol. Chem. *274*, 21797–21803.

Gietz, D., St. Jean, A., Woods, R.A., Schiestl, R.H. (1992). Improved method for high efficiency transformation of intact yeast cells. Nucleic Acid Res. *20*, 1425.

Glick, B.S., and Rothman, J.E. (1987). Possible role for fatty acyl-coenzyme A in intracellular protein transport. Nature *326*, 309–312.

Hechtberger, P., and Daum, G. (1995). Intracellular transport of inositol-containing sphingolipids in the yeast *Saccharomyces cerevisiae.* FEBS Lett. *367*, 201–204.

Kaiser, C.A., and Schekman, R. (1990). Distinct sets of SEC genes govern transport vesicle formation and fusion early in the secretory pathway. Cell *61*, 723–733.

Knudsen, J. (1979). Medium-chain fatty acid synthesis in lactating-rabbit mammary gland: intracellular concentration and specificity of medium-chain acyl thioester hydrolase. Biochem. J. *181*, 267–274.

Knudsen, J., Faergeman, N.J., Skott, H., Hummel, R., Borsting, C., Rose, T.M., Andersen, J.S., Hojrup, P., Roepstorff, P., and Kristiansen, K. (1994). Yeast acyl-CoA-binding protein: acyl-CoA-binding affinity and effect on intracellular acyl-CoA pool size. Biochem. J. *302*, 479–385.

Kragelund, B.B., Hojrup, P., Jensen, M.S., Schjerling, C.K., Juul, E., Knudsen, J., and Poulsen, F.M. (1996). Fast and one-step folding of closely and distantly related homologous proteins of a four-helix bundle family. J. Mol. Biol. *256*, 187–200.

Kragelund, B.B., Knudsen, J., and Poulsen, F.M. (1999). Acyl-coenzyme A binding protein (ACBP). Biochim. Biophys. Acta *1441*, 150–161.

Leidich, S.D., Drapp, D.A., and Orlean, P. (1994). A conditionally lethal yeast mutant blocked at the first step in glycosylphosphatidylinositol anchor synthesis. J. Biol. Chem. *269*, 10193–10196.

Lester, R.L., Wells, G.B., Oxford, G., and Dickson, R.C. (1993). Mutant strains of *Saccharomyces cerevisiae* lacking sphingolipids synthesize novel inositol glycerophospholipids that mimic sphingolipid structures. J. Biol. Chem. *268*, 845–856.

Lihrmann, I., Plaquevent, J.C., Tostivint, H., Raijmakers, R., Tonon, M.C., Conlon, J.M., and Vaudry, H. (1994). Frog diazepam-binding inhibitor: peptide sequence, cDNA cloning, and expression in the brain. Proc. Natl. Acad. Sci. USA *91*, 6899–6903.

Mikkelsen, J., Witkowski, A., and Smith, S. (1987). Interaction of rat mammary gland thioesterase II with fatty acid synthetase is dependent on the presence of acyl chains on the synthetase. J. Biol. Chem. *262*, 1570–1574.

Nikawa, J., Hosaka, K., and Yamashita, S. (1993). Differential regulation of two myo-inositol transporter genes of *Saccharomyces cerevisiae*. Mol. Microbiol. *10*, 955–961.

Oh, C.S., Toke, D.A., Mandala, S., and Martin, C.E. (1997). ELO2 and ELO3, homologues of the *Saccharomyces cerevisiae* ELO1 gene, function in fatty acid elongation and are required for sphingolipid formation. J. Biol. Chem. *272*, 17376–17384.

Ovalle, R., Lim, S.T., Holder, B., Jue, C.K., Moore, C.W., and Lipke, P.N. (1998). A spheroplast rate assay for determination of cell wall integrity in yeast. Yeast *14*, 1159–1166.

Patton, J.L., and Lester, R.L. (1991). The phosphoinositol sphingolipids of *Saccharomyces cerevisiae* are highly localized in the plasma membrane. J. Bacteriol. *173*, 3101–3108.

Patton, J.L., and Lester, R.L. (1992). Phosphatidylinositol phosphate, phosphatidylinositol bisphosphate, and the phosphoinositol sphingolipids are found in the plasma membrane and stimulate the plasma membrane H(+)-ATPase of *Saccharomyces cerevisiae*. Arch. Biochem. Biophys. *292*, 70–76.

Patton-Vogt, J.L., Griac, P., Sreenivas, A., Bruno, V., Dowd, S., Swede, M.J., and Henry, S.A. (1997). Role of the yeast phosphatidylinositol/phosphatidylcholine transfer protein (Sec14p) in phosphatidylcholine turnover and INO1 regulatiou. J. Biol. Chem. *272*, 200873–20883.

Pfanner, N., Glick, B.S., Arden, S.R., and Rothman, J.E. (1990). Fatty acylation promotes fusion of transport vesicles with Golgi cisternae. J. Cell Biol. *110*, 955–961.

Pfanner, N., Orci, L., Glick, B.S., Amherdt, M., Arden, S.R., Malhotra, V., and Rothman, J.E. (1989). Fatty acyl-coenzyme A is required for budding of transport vesicles from Golgi cisternae. Cell *59*, 95–102.

Puoti, A., Desponds, C., and Conzelmann, A. (1991). Biosynthesis of mannosylinositolphosphoceramide in *Saccharomyces cerevisiae* is dependent on genes controlling the flow of secretory vesicles from the endoplasmic reticulum to the Golgi. J. Cell Biol. *113*, 515–525.

Pusch, W., Balvers, M., Hunt, N., and Ivell, R. (1996). A novel endozepine-like peptide (ELP) is exclusively expressed in male germ cells. Mol. Cell. Endocrinol. *122*, 69–80.

Rasmussen, J.T., Rosendal, J., and Knudsen, J. (1993). Interaction of acyl-CoA binding protein (ACBP) on processes for which acyl-CoA is a substrate, product or inhibitor. Biochem. J. *292*, 907–913.

Robinson, C.V., Chung, E.W., Kragelund, B.B., Knudsen, J., Aplin, R.T., Poulsen, F.M., and Dobson, C.M. (1996). Probing the nature of noncovalent interactions by mass spectrometry: a study of protein-CoA ligand binding and assembly. J. Am. Chem. Soc. *118*, 8646–8653.

Rosendal, J., Ertbjerg, P., and Knudsen, J. (1993). Characterization of ligand binding to acyl-CoA-binding protein. Biochem. J. *290*, 321–326.

Rothman, J.E., and Wieland, F.T. (1996). Protein sorting by transport vesicles. Science *272*, 227–234.

Rothstein, R.J. (1983). One-step gene disruption in yeast. Methods Enzymol. *101*, 202–211.

Schjerling, C.K., Hummel, R., Hansen, J.K., Borsting, C., Mikkelsen, J.M., Kristiansen, K., and Knudsen, J. (1996). Disruption of the gene encoding the acyl-CoA-binding protein (ACB1) perturbs acyl-CoA metabolism in *Saccharomyces cerevisiae*. J. Biol. Chem. *271*, 22514–22521.

Schmidt, A., Wolde, M., Thiele, C., Fest, W., Kratzin, H., Podtelejnikov, A.V., Witke, W., Huttner, W.B., and Soling, H.D. (1999). Endophilin I mediates synaptic vesicle formation by transfer of arachidonate to lysophosphatidic acid. Nature *401*, 133–141.

Schneiter, R., Brugger, B., Sandhoff, R., Zellnig, G., Leber, A., Lampl, M., Athenstaedt, K., Hrastnik, C., Eder, S., Daum, G., et al. (1999). Electrospray ionization tandem mass spectrometry (ESI-MS/MS) analysis of the lipid molecular species composition of yeast subcel-

lular membranes reveals acyl chain-based sorting/remodeling of distinct molecular species en route to the plasma membrane. J. Cell Biol. 146, 741–754.

Schneiter, R., Hitomi, M., Ivessa, A.S., Fasch, E.V., Kohlwein, S.D., and Tartakoff, A.M. (1996). A yeast acetyl coenzyme A carboxylase mutant links very-long-chain fatty acid synthesis to the structure and function of the nuclear membrane-pore complex. Mol. Cell. Biol. *16*, 7161–7172.

Schonbachler, M., Horvath, A., Fassler, J., and Riezman, H. (1995). The yeast spt14 gene is homologous to the human PIG-A gene and is required for GPI anchor synthesis. EMBO J. *14*, 1637–1645.

Serrano, R. (1988). H^+-ATPase from plasma membranes of *Saccharomyces cerevisiae* and *Avena sativa* roots: purification and reconstitution. Methods Enzymol. *157*, 533–544.

Sumper, M., and Trauble, H. (1973). Membranes as acceptors for palmitoyl CoA in fatty acid synthesis. FEBS Lett. *30*, 29–34.

Sutterlin, C., Doering, T.L., Schimmoller, F., Schroder, S., and Riezman, H. (1997). Specific requirements for the ER to Golgi transport of GPI-anchored proteins in yeast. J. Cell Sci. *1997 110*, 2703–2714.

Toke, D.A., and Martin, C.E. (1996). Isolation and characterization of a gene affecting fatty acid elongation in *Saccharomyces cerevisiae*. J. Biol. Chem. *271*, 18413–18422.

Wach, A., Brachat, A., Pohlmann, R., and Philippsen, P. (1994). New heterologous modules for classical or PCR-based gene disruptions in *Saccharomyces cerevisiae*. Yeast *10*, 1793–1808.

Weigert, R., Siletta, M.G., Spano, S., Turacchio, G., Cericola, C., Colanzi, A., Senatore, S., Mancini, R., Polishchuck, E.V., Salmona, M., Facchiano, F., Burger, K.N., Mironav, A., Luini, A., and Corda, D. (1999). CtBP/BARS induces fission of Golgi membranes by acylating lysophosphatidic acid. Nature *402*, 429–433.

Wright, R., Basson, M., D'Ari, L., and Rine, J. (1988). Increased amounts of HMG-CoA reductase induce "karmellae": a proliferation of stacked membrane pairs surrounding the yeast nucleus. J. Cell Biol. *107*, 101–114.